Journal of Chemical Health Risks
www.jchr.org
JCHR (2025) 15(3), 60-69 | ISSN:2251-6727

Electrochemical Sensing of Dopamine at Polyaniline- Fe_3O_4 Modified Glassy Carbon Electrode and their Excellent Electromagnetic Interference Shielding Properties

Nydile. T. N[1], J. Sannappa[1*], G. Krishnamurthy[2], Malathesh Pari[3]

[1,1*]Department of PG Studies and Research in Physics, Kuvempu University Shankaraghatta, 577451, (Karnataka) India

[2,3] Department of PG studies and Research in Industrial Chemistry, Sahyadri Science College Shimoga,577203, (Karnataka) India

(Received: 16 March 2025 Revised: 20 April 2025 Accepted: 01 May2025)

KEYWORDS

Polyaniline, Fe_3O_4, EMI Shielding, Cyclic Voltametry, Dopamine

ABSTRACT:

In this work, Electrochemical detection of Dopamine and EMI Shielding behavior of PANI-Fe_3O_4 studied. The polyaniline doped Fe_3O_4 nanocomposite synthesized by in-situ polymerization. The spectroscopic characterization of samples carried out using various techniques such as FTIR, SEM, TGA and XRD techniques. The variation of EMI Shielding effectiveness of PANI- Fe_3O_4 studied with the help of Vector Network Analyzer in X-band region (8.2–12.4 GHz). The total EMI blocking efficiency for PANI sample found to be ~ -14 dB, and the blocking efficiency of PANI is found to be further improved with the embedment of Fe_3O_4 nanoparticles. Also the PANI/ Fe_3O_4/GC electrode express good sensing performance for Dopamine. Further PANI/ Fe_3O_4/GCE shows excellent long linear range, sensitivity and LOD are 100 to 1200 µM/L, 0.00143 and 66.666 and R^2 is 0.9978. Also this sensor shows repeatability and stability without leaching property.

1. Introduction

In the era of recent modern technologies and the demand of high-speed, high-efficient communication systems, the satellite communication, disaster surveillances, wireless technologies, accident and mobile phones etc., are increasing exponentially. To balance with daily life needs, modern electronic devices are developed with the high-frequency radiation devices. The nuisance of electromagnetic (EM) pollution has increased more significantly in two decades[1]. Hence Electromagnetic shielding applications are very much important to protect human health and electronic devices against hazardous effects of these electromagnetic radiation [2]. Materials, like intrinsically conducting polymers(ICPs) such as Polyaniline (PANI) are capable to reflect as well as absorb electromagnetic waves, and exhibits various advantages over metallic materials, such as light weight, less cost, easy preparation, good environmental resistance, greater optical and electronic property[3]. Also, alternatively used in several applications like electromagnetic interference (EMI) shielding, rechargeable battery etc,[4-8] The PANI nanocomposites containing Fe_3O_4 nanoparticles are mostly studied as the PANI having both electrical and magnetic characteristics[9]. The integration of Fe_3O_4 nanoparticles into the conductive PANI matrix is expected to form a heterogeneous hybrid system expressing the novel electromagnetic functionalities. The studies illustrating the usage of novel PANI/ Fe_3O_4 nanocomposites provides considerable EMI shielding over X-Band [6-10]. Furthermore, Dopamine (DA), a monoamine neurotransmitter (NT) plays a major role in functioning of central, renal nervous and hormonal systems. The abnormal concentration of DA serves as a crucial indicator for the human health problems like Huntington's, Alzheimer's and Parkinson's diseases [32]. The treatment of such diseases necessitates the accurate determination of DA in biological samples because of its less concentration in brain and its major action depending on the overall levels and short burst, which makes its detection a challenging role [33-34]. The electrochemical analysis is the most effective and reliable technique because of its excellent results

Journal of Chemical Health Risks
www.jchr.org
JCHR (2025) 15(3), 60-69 | ISSN:2251-6727

reproducibility, high sensitivity, low cost of operation and wide selectivity [35]. However, the DA overlapped oxidation potential with other biomolecules like uric acid (UA) and ascorbic acid (AA) hindered the electrochemical sensing of DA. Therefore, to overcome this issue by modifying an electrode with suitable materials for an efficient way to enhance the electrode sensitivity and selectivity [36,38]. The Fe_3O_4 nanoparticle attracted more attention due to their simplicity in the synthesis method, high electrical conductivity, chemical stability, non-toxicity, good catalytic behavior and low cost [37]. which plays a important role in their uses in field of electrochemistry. The main aim of this analysis was to synthesize and compare the electrochemical behavior of Fe_3O_4 nanoparticles doped with PANI (i.e., PANI- Fe_3O_4) and further it is characterized to affirm their microstructural characteristics[38,39]. Also, the detection of DA with synthesized nanocomposite was attempted.

2. Materials and Methods

The chemicals, reagents and solvents are used of high-grade quality and were used as such without further purification obtained from Sigma Aldrich. **2.1 Preparation of Fe_3O_4 Nanoparticles:**

Fe_3O_4 nanoparticles synthesized by coprecipitation method. FeCl3.6H2O (5.20 g, 0.02 mol) and $(NH4)_2$ $Fe(SO4)_2$ .6H2O (3.52 g, 0.01 mol) were dissolved in 50 mL of deionised water. NaOH 3M solution added dropwise into the iron solution[7]. Then, the reaction mixture was heated at 60 °C with a constant stirring for 1 hour. Fe_3O_4 nanoparticles were obtained as black precipitates. The products were separated from the solution using external magnetic field and washed using distilled water until neutral pH to remove impurities. Furthermore, Fe_3O_4 was dried at 80^0 C for 16 hours and continued at 100^0 C for 4 hours[8].

2.2 Preparation of PANI/ Fe_3O_4 NCs:

PANI-Fe_3O_4 nanocomposite synthesized through in-situ polymerization method using ammonium persulfate (APS) as oxidant without the support of surfactants [9]. The synthesis procedure is as followed: 0.61 mol/L aniline into polymerization vessel consisting Fe_3O_4 in 100 ml of 1.13 mol/L H2SO4 acid solution at normal room temperature and continuous magnetic stirring for 2h.Then 50 ml (1M) of Ammonium Per Sulfate $(NH4)2S_2O_8$ added slowly to above reaction mixture. Then it is filtered and washed with distilled water and methanol. The resultant product dried in oven at 70^0 C for 24h to get green–black powder of PANI – Fe_3O_4 nanocomposite**[**10].

2.3 Detection Method

EMI shielding effectiveness of sample can be obtained using Vector Network Analyser at CIF & CMFF IIT Palakkad. FTIR Spectra were reported using Shimadzu Spectrometer, TGA of sample was found by SDT Q600 in a N_2 atmosphere at USIC, Karnartaka University Dharwad (KUD). SEM analysis of sample was obtained by JSM-IT500 at SAIF in KUD. XRD analysis was found by single crystal XRD at Tumkur University. The CV were carried out using CHI1608D electrochemical workstation (USA) at SSC shimoga.

3. RESULTS AND DISCUSSION

3.1. FTIR Spectroscopy

The FT-IR spectra were used to determine the chemical structure and functional groups of synthesized samples. **Fig.-1**. Shows FT-IR characteristic peaks of (a) Fe_3O_4 nanoparticles (b) PANI and (c) PANI- Fe_3O_4 nanocomposites . The short peak in 1620 cm−1 can be correlated to the different modes of bonded water molecules existing in the ferrofluid while the prominent peaks at 452 and 690 cm−1, are due to the stretching and torsional vibration modes of Fe-O bonds in tetrahedral and octahedral sites, respectively. Furthermore, FT-IR spectrum of PANI exhibits characteristic peaks at 3109 cm-1 due to N–H stretching vibrations of amino groups. The bands at about 1614 and 1352 cm-1 arise because of quinoid rings and benzenoid ring units [12]. The existence of all these bands in **Fig. 1c** clearly indicating that PANI is composed of both imine and the amine units. The peak appeared at 642 cm−1 in nanocomposite is ascribed to Fe–O stretching band of Fe_3O_4. The noticed shift on bands at 490 and 543 cm-1 confirmed the introduction of Fe_3O_4 in PANI[11].

Journal of Chemical Health Risks
www.jchr.org
JCHR (2025) 15(3), 60-69 | ISSN:2251-6727

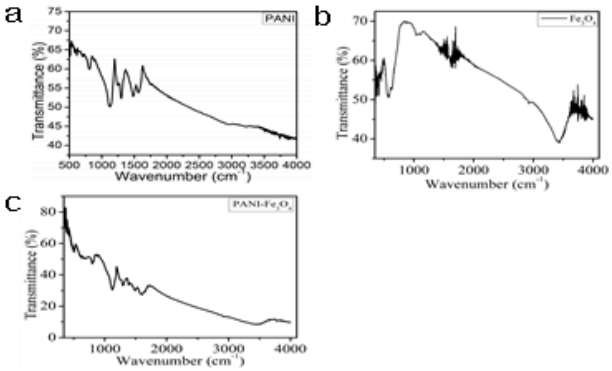

Fig.-1: FTIR of a. PANI b. Fe_3O_4 nanoparticles and c. PANI- Fe_3O_4 nanocomposite

3.2. S
EM analysis:

Fig.-2 shows SEM microphotographs of (a) PANI (b) Fe_3O_4 and (c) PANI- Fe_3O_4 nanocomposite. It can be seen from **Fig.-2**, PANI shows that all particles are agglomerated irregular along some are spherical in nature [14]. While the PANI– Fe_3O_4 consists of granular particles. Small irregular nanostructured Fe_3O_4 nanoparticles dispersed on surface of PANI matrix. The agglomeration of Fe_3O_4 on PANI matrix confirms the formation of nanocomposite [13].

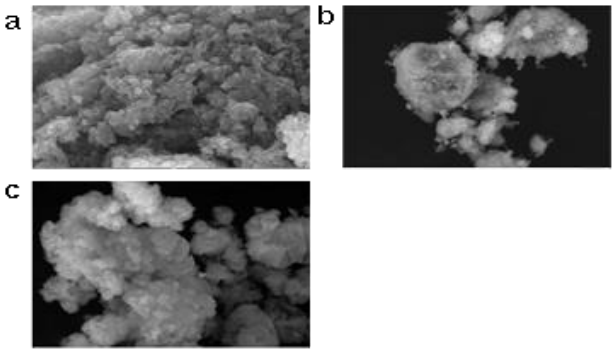

Fig.-2: SEM images of a. PANI, b. Fe_3O_4 and c. PANI- Fe_3O_4 nanocomposite

3.3. XRD Analysis:

The structural investigation of the PANI, Fe_3O_4 and PANI-Fe_3O_4 were studied by powder X-ray diffraction (XRD) shown in **Fig.-3(a,b,c).** The XRD pattern of Fe_3O_4 shows spinel structure with diffraction peaks at $2\Theta = 30.62^0$, 35.22^0, 44.06^0, 56.10^0 and 64.07^0. The XRD spectra of PANI has broad peak in the range $2\Theta = 23\text{-}26^0$ and a small peak at $2\Theta = 22.08^0$ exhibiting amorphous nature. **Fig.-3c**. shows XRD spectral pattern of PANI- Fe_3O_4 nanocomposite are very likely to that of PANI. It is exhibiting a broad peak at $2\Theta = 22.5^0$ also peaks at $2\Theta = 25.2^0$, 30.14^0 confirming the formation of PANI- Fe_3O_4 nanocomposite[14,15].

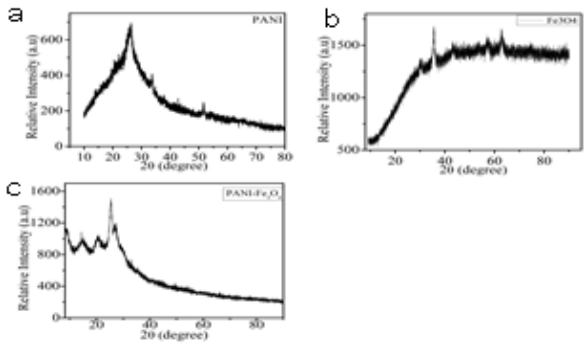

Fig.-3: XRD of a. PANI b. Fe_3O_4 nanoparticles and c. PANI- Fe_3O_4nanocomposite

3.4. TGA analysis:

The TG thermogram of Fe_3O_4, PANI and PANI/ Fe_3O_4 NCs are shown in **Fig.-4.** Fe_3O_4 undergoes two steps degradation. The initial loss at 103 ◦C observed due to loss of adsorbed water. The second stage weight loss is due to decomposition of bounded ethylene glycol above 230 ◦C and afterward, above 460 ◦C there is no loss but we can observe the rise in curve, which may be due to the fact that thermal expansion of Fe_3O_4 at higher temperature. PANI shows three-step weight loss behavior[15]. The loss above 200 ◦C may be due to loss of SDBS and thermal oxidative degradation and decomposition of PANI started after 300◦C. PANI/Fe_3O_4 composite undergoes similar decomposition steps as that of PANI, but it has greater stability. The greater stability of composite may be because of the interaction between PANI and Fe_3O_4 which controls the thermal motion of PANI chain in composite and enhances the thermal stability of the composite[16-18].

Journal of Chemical Health Risks
www.jchr.org
JCHR (2025) 15(3), 60-69 | ISSN:2251-6727

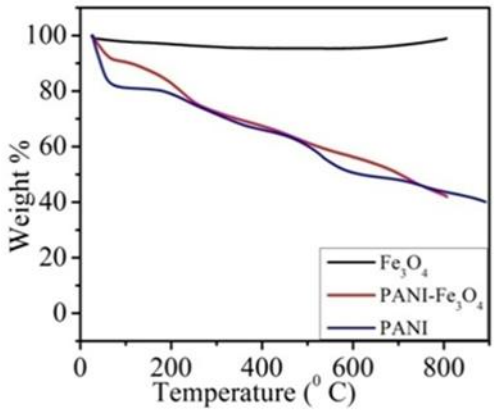

Fig.-4: TGA analysis of PANI, Fe_3O_4 and PANI-Fe_3O_4 nanocomposite

3.5. EMI shielding effectiveness:

The phenomenon of loss of electromagnetic radiations by the attenuating medium to protect the electronic devices from interference is known as electromagnetic interference shielding efficiency/effectiveness (EMI-SE)[18,19]. The composites of conducting and magnetic materials are more preferable due to their excellent shielding efficiency.[20,21] The total shielding efficiency (SE_T) of the attenuating medium can be expressed as the sum of reflection shielding efficiency (SE_R) and absorption shielding efficiency (SE_A): $SE_T = SE_R + SE_A$. The first component of Equation is the consequence of the mismatching of impedance at air–barrier interface, whereas the second component is resulting from the loss of incident EM radiation in the form of heat in the inside of shield [22,23]. These shielding efficiencies are also measured from the scattering parameters (S_{11}, S_{12}, S_{21} and S_{22}) of the EM wave using the VNA. In terms of scattering parameters, the coefficients A, R, and T can be expressed as [1]:

$$\left.\begin{aligned} R &= |S_{11} \text{ or } S_{22}|^2 \\ T &= |S_{12} \text{ or } S_{21}|^2 \\ A &= 1 - R - T \end{aligned}\right\} \quad (1)$$

$$SE_R = -10\log(1-R) \quad (2)$$

The EMI SE due to absorption is:

$$SE_A = -10\ \log\left(\frac{T}{1-R}\right) \quad (3)$$

The shielding efficiencies estimated from expressions 2 & 3 are drawn in **Fig.- 5, 6 & 7** with the variation in applied frequency. **Fig.-5** demonstrates the variation of absorption shielding efficiencies of the pure PANI and nanocomposite sample of PANI with Fe_3O_4 with applied frequency. This is perceived that absorption shielding efficiency for the prepared samples increases from 9 dB for pristine PANI to 18 dB for composite sample with loading concentration of Fe_3O_4. The enhancement in absorption shielding efficiency can be accredited to the rise in electric as well as magnetic dipoles in the bulk of attenuating medium and to enhancement in electrical conductivity and heterogeneity in composites[24]. **Fig.-6** illustrates the reflection shielding efficiencies for the PANI and PANI/ Fe_3O_4 nanocomposite sample, indicating the increase in reflection shielding efficiency with loading of Fe_3O_4 nanoparticles. The shielding efficiency of pure PANI is found to increase from 5 dB for pure PANI to 10.4 dB for PANI/ Fe_3O_4 nanocomposite with loading of Fe_3O_4 nanoparticles. The enhanced shielding efficiency with Fe_3O_4 nanoparticles loading concentrations may be indorsed to the enhancement in electrical conductivity of PANI composites and availability of free charge carriers for interaction with EM radiation at the air–barrier interfere for reflection[25,26]. **Fig.-7** shows the enhancement in total shielding efficiencies of PANI and PANI- Fe_3O_4 with applied frequency. It can be observed that total shielding efficiency (SET) of the prepared sample enhanced with the addition of Fe_3O_4 into PANI matrix[27].

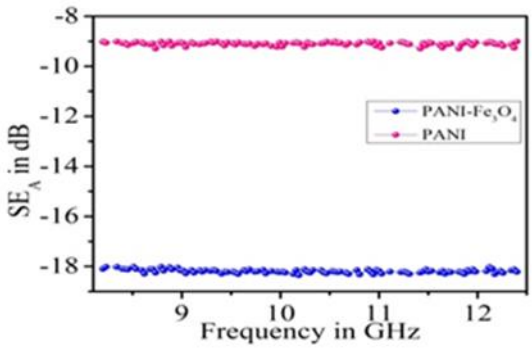

Fig.-5: SE_A of PANI and PANI- Fe_3O_4 nanocomposite

The observed values of SET for the pure PANI and nanocomposites are 14 and 28 dB respectively, at 8.2 GHz applied frequency, and these values are greater than the industrial standard of shielding effectiveness,

Journal of Chemical Health Risks
www.jchr.org
JCHR (2025) 15(3), 60-69 | ISSN:2251-6727

i.e., 12 dB for good attenuators. The significant contribution in the total shielding efficiency from the absorption loss as compared to reflection loss indicates the better device performance in extinction of EM radiation from environment instead of merely reflection in the environment from the device surface[24-28]. The comparative studies of EMI Shielding property of various reported materials under optimal conditions can be shown in **Table 1**.

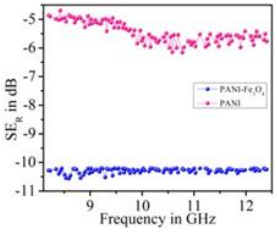

Fig 6

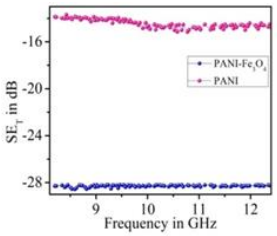

Fig 7

Fig.-6: SE_R of PANI and PANI- Fe_3O_4 nanocomposite

Fig.-7: SE_T of PANI and PANI- Fe_3O_4 nanocomposite

Table 1: comparative studies of EMI Shielding property of various reported materials under optimal conditions

Material	Frequency	SE_T (dB)	Thickness	Ref.
PANI-CuO (5%, 10%,15%)	8.2-12.4GHz	~ -18.2 to -23.1	2mm	**[27]**
MWCNT/CuO/Fe_3O_4/ Polyaniline	8.2- 18 GHz	~ -87.4	2mm	**[28]**
RGO/PANI /Cu_2O	2-18GHz	~ -52.8	2mm	**[29]**
Polyaniline/ V_2O_5	12-18GHz	~ 19	2mm	**[30]**
PANI/ Fe_3O_4	8.2-12.4GHz	~ -28	2mm	**Present work**

3.6. Electrochemical Characterization

3.6.1. Preparation of modified glassy carbon electrode

0.5 mg of PANI-Fe_3O_4/GCE taken in IPA (isopropanal) solvent were sonicated of 30 min and the 5 µL of the finely dispersed solution was drop coated on the previously cleaned and dried GCE and the electrode surface dried at normal room temperature under ambient conditions.

3.6.2. Electro catalytic behaviour of the different electrode

Electro catalytic activity of different electrodes, the electrochemical oxidation of the DA was accomplished in PBS (pH 7.0) via CV technique bearing 100 µM DA for the comparision of the bare electrode as depicted in **Fig.-8**. A bare GC electrode displayed linear peak wave and also a small peak current growth was observed when the DA was added to the buffer solution in the range of 0.5 V in presence of a surface modified GCE (curve b). quasi-reversible peaks were noticed on modified PANI-Fe_3O_4/GCE[29,30]. Upon comparing with bare GCE, about 12 times larger current signal was received from PANI-Fe_3O_4/GCE at around 0.5 V which confirmed that PANI-Fe_3O_4/GCE could notably promote oxidation of pesticide[32,40].

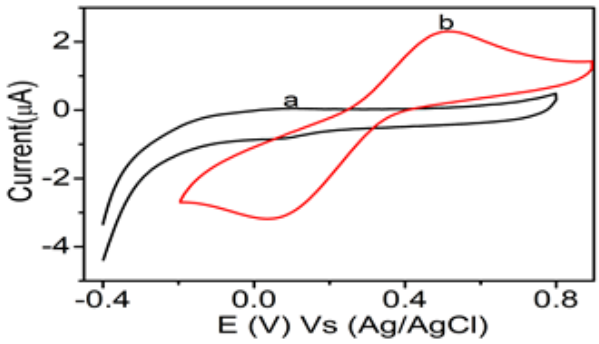

Fig.-8. CV of a) bare GCE b) PANI-Fe_3O_4/GCE with DA concentration of 100 µmol L− 1 in PBS at pH 7.0 at a scan rate of 50 mV s − 1 in N_2

3.6.3. Electrocatalytic behavior of PANI-Fe_3O_4/GC electrode towards DA

Electrochemical sensing of DA was examined utilizing PANI-Fe_3O_4/GCE which exhibited well-defined peaks at 0.5 V in the presence of varied amount of DA in PBS at pH 7.0 can be shown in **Fig.-9.** The peak current was

Journal of Chemical Health Risks
www.jchr.org
JCHR (2025) 15(3), 60-69 | ISSN:2251-6727

increases linearly when the concentration of DA rises from 100 to 1200 µmol L^{-1} with a sensitivity of 0.00143 $\mu A \mu M^{-1}$ mm^{-2}, LOD of 66.666 $\mu A \mu M^{-1}$ mm^{-2} and a linear regression equation Y = 0.00143x + 3.090, R^2 = 0.9978**[31,40].** The electrochemical property of the PANI-Fe_3O_4/GCE was compared with the bare GCE (Fig. 12(a)). According to the CV of modified electrodes, PANI-Fe_3O_4/GCE (0.5) displayed an appreciable electrocatalytic effect with enhanced peak current compared to the bare GCE[33].

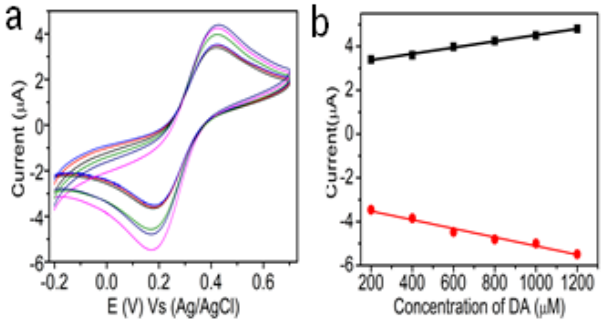

Fig.- 9. CVs of the PANI-Fe_3O_4/GC electrode in PBS (pH 7.0) with different concentrations of DA. Scan rate: 50 mV/s.

3.6.4. Effect of Scan Rate on electro catalytic capability of DA

CVs for DA in a PBS at PANI-Fe_3O_4/GC electrode showed a pair of quasi-reversible peaks shown in **Fig.-10**. There is a increase in oxidation peak current with increasing scan rate, in range from 50-100 mVs^{-1} the redox peak current is proportional to scan rate[34-36]. The plot of peak current vs scan rate for DA exhibited a linear relationship and the straight line equation is represented by Y= 0.0268(DA) - 0.1136 with correlation coefficient of R^2 =0.9731. The linear plot of peak current vs scan rate inferred that the electrode reaction is a adsorption-controlled process**[37-39].** Results presents that our PANI- Fe_3O_4/GCE modified electrodes has excellent stability, sensitivity and repeatability. PANI- Fe_3O_4/GCE synthesized compounds characterized by electrochemical and spectral methods. Also, the comparison of results for DA shown in **Table 2**.

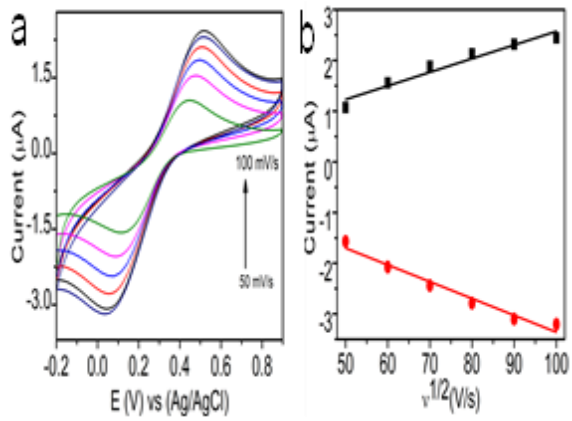

Fig.-10.(a) CV of dopamine at PANI-Fe_3O_4/GCE scanning rate ranging from (50 mV^{-1} to 100 mVs^{-1}). (b) Inset: Calibration graph of peak current vs scan rate

Table 2. Comparison of results for the DA with the literature reports

Electrode material	Linear range µM/L	Technique	LOD µM/L	Sensitivity	Reference
rGO-Zn(II) TPEBiPc	0.02-1.0	CV	0.006	2.8784	**[32]**
poly(l-arginine)/CPE	50-100	CV	0.5	-	**[31]**
PANI-CuO/GCE	10 – 130	CV	3.666	0.0153	**[27]**
PANI-Fe_3O_4 GCE	100-1200	CV	66.666	0.00143	**This work**

Journal of Chemical Health Risks
www.jchr.org
JCHR (2025) 15(3), 60-69 | ISSN:2251-6727

3.6.5. Determination of Real Sample Analysis

The relevance of modified GCE as electrochemical sensor conducted for the effective detection of DA in Pharmaceutical drug, DA hydrochloride solution. The measurement of concentration of DA hydrochloride in solution done by applying a calibration plot with the methods suggested in effect of concentration in standard DA. Results obtained after the standard addition procedure shown in **Table 3**. The Recoveries from 97 to 105.5% of DA secured for dopamine hydrochloride samples (n = 5 repetitions). It is a evident of accuracy of the suggested procedure. Statistical calculations for aquired outputs depicted excellent precision for CV method, showing PANI-Fe_3O_4/GC modified electrode used for sensing of dopamine hydrochloride solution samples[31,38].

Table 3. Determination of DA in dopamine hydrochloride solution

No	Spiked DA (mg)	Found DA (mg)	Recovery	RSD %
1	4	3.87	97.25	2.42
2	4	4.18	105	3.32
3	4	3.8	95	2.2
4	4	4.08	101	2.66
5	4	3.89	97.5	2.47

4. CONCLUSION

The synthesis of PANI-Fe_3O_4carried out by in-situ chemical polymerization reaction. The spectroscopic characterization of synthesized samples can be done using FTIR, XRD, SEM and TGA techniques. The PANI-Fe_3O_4 exhibits semi-crystalline nature and the semi-crystallanity of Fe_3O_4 nanoparticles are not disturbed in the PANI matrix. The synthesized composite exhibits a very good thermal stability. The EMI SE of nanocomposite in X-band indicating that synthesized samples exhibits excellent EMI SE of -28 dB. Also, incorporation of Fe_3O_4 on PANI matrix affects the EMI SE value. As the concentration of Fe_3O_4 nanoparticles on PANI increases the EMI SE also increases. Hence, the synthesized nanocomposites can be potent EMI shielding materials in various electronic devices and applications. Furthermore, PANI-Fe_3O_4 /GCE can be used in the detection and sensing of Dopamine.. Additionally, PANI-Fe_3O_4 /GCE used in the detection and sensing of Dopamine also in the real samples i.e., Dopamine hydrochloric solution. All these results indicates PANI-Fe_3O_4 can be an excellent EMI shielding material with a high sensing performance of Dopamine.

Refrences

1. Manjunatha Kumara, K.S.; Shivakumar, P.; Shubhankar Kumar Bose; Nagaraju, D.H.; Hydrogels of PANI doped with Fe3O4 and GO for highly stable sensor for sensitive and selective determination of heavy metal ions. Inorganic Chemistry Communications. (2023), 158(1). https://doi.org/10.1016/j.inoche.2023.111553.
2. Panigrahi, R.; Srivastava, S.; Trapping of microwave radiation in hollow polypyrrole microsphere through enhanced internal reflection: A novel approach. Scientific reports. (2015), 5. https://doi.org/10.1038/srep07638.
3. Zou, L.; Zhang, S.; Li, X.; Lan, C.; Step-by-Step Strategy for Constructing Multilayer Structured Coatings toward High-Efficiency Electromagnetic Interference Shielding. Advanced Materials Interfaces. (2016), 3(5). https://doi.org/10.1002/admi.201500476.
4. Rayar, A.; Naveen, C.S.; Onkarappa, H.S.; Betageri, V.S.; EMI shielding applications of PANI-Ferrite nanocomposite materials: A review. Synthetic Metals. (2023), 295. https://doi.org/10.1016/j.synthmet.2023.117338.
5. Kulkarni, G.; Jadhav, S.; Patil, K.; Patil, P.; α-MnO2 nanorods-polyaniline (PANI) nanocomposites synthesized by polymer coating and grafting approaches for screening EMI pollution. Ceramics International. (2021), 47. https://doi.org/10.1016/j.ceramint.2021.02.061.
6. Mohan, R.; Ayyappan, A.; Mani, M.; Varma, S.; Sankaran, J.; Nano CuO-embedded polyaniline films as efficient broadband electromagnetic shields. Material Chemistry & Physics. (2022), 290. https://doi.org/10.1016/j.matchemphys.2022.126647.

7. Jannah, R.; Onggo, D.; Synthesis of Fe3 O4 nanoparticles for colour removal of printing ink solution. Journal of Phyicss: Conference Series. (2019), 1245. https://doi.org/10.1088/1742-6596/1245/1/012040.
8. Patil, M.: Khairnar, S.; Shrivastava, V.; Synthesis, characterisation of polyaniline–Fe3O4 magnetic nanocomposite and its application for removal of an acid violet 19 dye. Applied Nanoscience. (2015), 6. 10.1007/s13204-015-0465-z.
9. Li, X.; Zhang, G.; Wang, B.; Lin, T.; Wang, G.; One-pot synthesis of polyaniline/Fe 3 O 4 nanocomposite in ionicliquid: electrical conductivity and magnetic studies. E3S Web of Conferences. (2019), 118. https://doi.org/10.1051/e3sconf/201911801059.
10. Umare, S.S.; Shambharkar, B.H.; Ningthoujam, R.S.; Synthesis and characterization of polyaniline–Fe3O4 nanocomposite: Electrical conductivity, magnetic, electrochemical studies. Synthetic Metals. (2010),160. https://doi.org/10.1016/j.synthmet.2010.06.015.
11. Goswami, B.; Mahanta, D.; Polyaniline-Fe3O4 and polypyrrole-Fe3O4 magnetic nanocomposites for removal of 2, 4-dichlorophenoxyacetic acid from aqueous medium. Journal of Environmental Chemical Engineering. (2020), 8(4). https://doi.org/10.1016/j.jece.2020.103919.
12. Shoaib-ur-Rehman, M.; Javaid, ZAsghar, I.; Azam, M.; Photo-catalytic response of zinc-doped nickel ferrite nanoparticles for removal of chromium from industrial wastewater. IOP Conference Series: Material Science & Engineering. (2020), 863. https://doi.org/10.1088/1757-899X/863/1/012017.
13. Butoi, B.; Ciobanu, C.S.; Iconaru, S.L.; Negrilă, C.C.; Badea, M.A.; Balas, M; Iron-Oxide-Nanoparticles-Doped Polyaniline Composite Thin Films. Polymers. (2022), 14(9). https://doi.org/10.3390/polym14091821.
14. Gholampour, M.; Movassagh-Alanagh, F.; Salimkhani, H.; Fabrication of nano-Fe3O4 3D structure on carbon fibers as a microwave absorber and EMI shielding composite by modified EPD method. Solid State Sciences. (2016), 64. https://doi.org/10.1016/j.solidstatesciences.2016.12.005.
15. Kadar, C.; Faisal, M.; Narasimha, R.; Maruthi, N.; Enhancing electromagnetic interference shielding effectiveness (EMI SE) of anticorrosive polypyrrole/zinc tungstate composites: multifunctional approach. Journal of Material Science: Materials in Electronics. (2022), 33. https://doi.org/10.1007/s10854-022-08348-w.
16. Mamatha, G.M.; Dixit, P.; Hari Krishna, R.; Girish Kumar, S.; Polymer based composites for electromagnetic interference (EMI) shielding: The role of magnetic fillers in effective attenuation of microwaves, a review. Hybrid Advance. (2024), 6. https://doi.org/10.1016/j.hybadv.2024.100200.
17. Darvishzadeh, A.; Nasouri, K.; Structural engineering of nickel-coated carbon fibers with high electrical conductivity for flexible EMI shielding. Journal of Material Science: Materials in Electronics. (2022), 33. https://doi.org/10.1007/s10854-022-07751-7.
18. Ruchi, Gupta, V.; Dalal, R.; Goyal, S.L.; Electromagnetic interference shielding performance of in-situ polymerized PANI/Fe3O4 nanocomposites in X-band frequency range. Polymer Bulletin. (2023), 81. https://doi.org/10.1007/s00289-023-04950-y.
19. Wang, Z.; Wu, L.; Lina, Z.; Zhou, J.; Jiang, Z.; Shen, B.; Chemoselectivity-induced multiple interfaces in MWCNT/Fe_3O_4@ZnO heterotrimers for whole X-band microwave absorption. Nanoscale. (2014). 21. https://doi.org/10.1039/c4nr03040k.
20. Ting, T.H.; Yu, R; Jau, Y.; Synthesis and microwave absorption characteristics of polyaniline/NiZn ferrite composites in 2–40 GHz. Material Chemistry and Physics. (2011), 126. https://doi.org/10.1016/j.matchemphys.2010.11.011.
21. Yang, Y.; Gupta, M.; Dudley, K.; Lawrence, R.; Novel Carbon Nanotube−Polystyrene Foam Composites for Electromagnetic Interference Shielding. Nano letters. (2005), 5. **https://dx.doi.org/10.21741/9781945291876-6**
22. Zhong, Y.; Guo, Y.; Li, M.; Wei, X.; Wang, J.; A hollow hybrid separated structure based on Ni/Pani-Fe3O4 constructed for an ultra-efficient electromagnetic interference shielding and hydrophobic PPTA fabric. Journal of Alloys &

Compounds.(2022),925. https://doi.org/10.1016/j.jallcom.2022.166666

23. Pal, R.; Goyal, S.; Rawal, I.; Gupta, A; Tailoring of EMI shielding properties of polyaniline with MWCNTs embedment in X-band (8.2–12.4 GHz). Journal of Physics & Chemistry of Solids. (2022), 169. http://dx.doi.org/10.1016/j.jpcs.2022.110867

24. Zhang, J.; Li, J.; Tan, G.; Hu, R.; Wang, J; Chang, C; Wang, X; Thin and Flexible Fe–Si–B/Ni–Cu–P Metallic Glass Multilayer Composites for Efficient Electromagnetic Interference ShieldingACS Applied Materials & Interfaces. (2017), 48. https://doi.org/10.1021/acsami.7b12504

25. Wang, G.S; Zhu, J.Q; Guo, A.P.; Ao-Ping, W.; Shan-Wen, G.; Lin & Qu; Juan, X; Improved microwave absorption and electromagnetic interference shielding properties based on graphene–barium titanate and polyvinylidene fluoride with varying content. Materials Chemistry Frontier. (2017), 1. https://doi.org/10.1039/C7QM00204A

26. Feng, Y.; Li, W.; Yafei, H; Yu, Y; Cao, W.P; Zhang, T.; Fei, W.; Positive/negative electrocaloric effect induced by defect dipoles in PZT ferroelectric bilayer thin films. Journal of Materials Chemistry C. (2014), 3. http://dx.doi.org/10.1039/C6RA14776C

27. Nydile, T.N.; Sannappa, J.; Pari, M.; Vasantakumarnaik, N.K,; Shet, R.; Madhura, R; Polyaniline Ingrained Copper Oxide (PANI/CuO) Nanocomposites for Effective Electromagnetic Interference Shielding and Their Sensitive Detection of Dopamine. Analytical & Bioanalytical Electrochemistry. (2024), 16(7). https://doi.org/10.22034/abec.2024.714686.

28. Afzali, S.S.; Hekmatara, H.; Seyed-Yazdi, J.; hosseini, M.; bagher, S. M.; Tuned MWCNT/CuO/Fe3O4/Polyaniline nanocomposites with exceptional microwave attenuation and a broad frequency band. Scientific Reports, (2022), 12. https://doi.org/10.1038/s41598-022-13210-4.

29. Yan, P.; Miao, J.; Cao, J.; Zhang, H.; Wang, C.; Xie, A.; Facile synthesis and excellent electromagnetic wave absorption properties of flower-like porous RGO/PANI/Cu2O nanocomposites. Journal of Materials Science. (2017), **52.** https://doi.org/10.1007/s10853-017-1418-6.

30. Maruthi, N.; Faisal, M.; Narasimha, R.; Polyaniline/V_2O_5 composites for anticorrosion and electromagnetic interference shielding Materials Chemistry & Physics. (2021), 259. https://doi.org/10.1016/j.matchemphys.2020.124059

31. Chandrashekar, B.N.; Swamy, K.; Pandurangachar, M.; Sathisha, T.V.; Sherigara, B.; Electropolymerisation of L-arginine at carbon paste electrode and its application to the detection of dopamine, ascorbic and uric acid. Colloids and surfaces –B. (2011), 88. https://doi.org/10.1016/j.colsurfb.2011.07.023

32. Pari, M.; Venugopala Reddy, K.R.; Fassiulla, Chandrakala, K.B.; Amperometric determination of dopamine based on an interface platform comprising tetra-substituted Zn2+ phthalocyanine film layer with embedment of reduced graphene oxide. Sensors & Actuators A. (2020),316. https://doi.org/10.1016/j.sna.2020.112377

33. Afroz, L.; Moinuddin Khan, M.H.; Vagdevi, H.M.; Pari, M.; Mohammed Shafeeualla, R.; Mussuvir Pasha, K.M.; nvestigation on Co(II), Ni(II), Cu(II) and Zn(II) complexes derived from novel N′-(3-hydroxybenzoyl)thiophene-2-carbohydrazide: structural characterization, electrochemical detection of biomolecules, molecular docking and biological evaluation. Emergent Materials. (2021), 5. http://dx.doi.org/10.1007/s42247-021-00312-4

34. Kumar, P.S.; Sreeja, B. S.; Kumar, K. K.; Padmalaya, G.; Investigation of Nafion coated GO-ZnO nanocomposite behaviour for sulfamethoxazole detection using cyclic voltammetry. Food and Chemical Toxicology. (2022),167. https://doi.org/10.1016/j.fct.2022.113311

35. Jill Venton, B.; Cao, Q.**;** Fundamentals of fast-scan cyclic voltammetry for dopamine detection. Analyst-RSC. (2020), 145(4). https://doi.org/10.1039/C9AN01586H

36. Chelly, S.; Chelly, M.; Zribi R.; Neri, G.; Electrochemical Detection of Dopamine and Riboflavine on a Screen-Printed Carbon Electrode Modified by AuNPs Derived from *Rhanterium suaveolens* Plant Extract. ACS Omega. (2021), 6 (37). https://doi.org/10.1021/acsomega.1c00793
37. Manbohi, A.; Ahmadi, S.H.; Sensitive and selective detection of dopamine using electrochemical microfluidic paper-based analytical nanosensor. Sensing & Bio-Sensing Research. (2019), 23. http://dx.doi.org/10.1016/j.sbsr.2019.100270
38. Mokole, S.J.; Aliyu, A.; Fayemi, O.E.; Electrochemical detection of dopamine using green and chemical synthesized CuO/PANI nanocomposite modified electrode. Applied Physics A. (2023), 129. https://doi.org/10.1007/s00339-023-06438-y
39. Ranku, M.N.; Uwaya G.E.; Fayemi, O.E; Electrochemical Detection of Dopamine at Fe3O4/SPEEK Modified Electrode. Molecules. (2021),26.https://doi.org/10.3390/molecules26175357
40. Zahid, M.; Anum, R.; Siddique, S.; Shakir H.M.F.; Rehan, Z.; Electromagnetic interference shielding study in microwave and NIR regions by highly efficient Ag/ZnS and polyaniline-Ag/ZnS particles.J. ThermoPlastic Composite Mater. (2021), 36. http://dx.doi.org/10.1177/08927057211064990